GEOPHYSICS, VOL. 73, NO. 6 (NOVEMBER-DECEMBER 2008); P. V47–V53, 7 FIGS.
10.1190/1.2985822

Convergence of the two-point correlation function toward the Green's function in the context of a seismic-prospecting data set

Pierre Gouédard[1], Philippe Roux[1], Michel Campillo[1], and Arie Verdel[2]

ABSTRACT

When considering direct waves in the correlation process, the Green's function is reconstructed when using an even distribution of seismic sources or when the source distribution is restricted to the direction close to the alignment of the sensors. On the other hand, when considering records of coda waves, the convergence is achieved for any source distribution, as expected theoretically. We extract the expected amplitude decay along a seismic profile from the correlation functions when an even distribution of sources is considered or when the time window includes scattered waves.

INTRODUCTION

The Green's function of a medium between points A and B represents the record we would get at A if an impulse source were applied at B. In the case of random isotropic noise sources, the crosscorrelation of wavefields recorded at two points converges to the Green's function of the medium, including all reflection, scattering, and propagation modes. Various experimental, numerical, and theoretical approaches have been developed to demonstrate this result and to define more precisely under which assumption it is valid.

Aki (1957) proposed to use seismic noise to retrieve, frequency by frequency, the dispersion properties of surface waves in the subsoil. Later, helioseismology was the first field to use ambient noise crosscorrelation in the time domain for imaging. The recordings of random motion of the solar surface were processed to retrieve time-distance information on the solar subsurface (Duvall et al., 1993; Gilles et al., 1997; Rickett and Claerbout, 1999). The same idea developed as Claerbout (1968) proposed using daylight imaging in geophysical prospecting.

More recently, a seminal paper by Weaver and Lobkis (2001) shows how diffuse thermal noise recorded and crosscorrelated at two ultrasonic transducers, working at megahertz frequencies and fastened to one face of a duralumin cube 10 cm on a side, provides the complete time-domain Green's function between these two points. This spectacular result has been the start of a complete revival of the subject because experimental evidence of ambient noise crosscorrelations have been demonstrated in acoustics and elastic plates (Lobkis and Weaver, 2001; Weaver and Lobkis, 2001; Larose et al., 2004; Larose et al., 2007; Sabra et al., 2008); seismology (Paul and Campillo, 2001; Campillo and Paul, 2003; Schuster et al., 2004; Shapiro and Campillo, 2004), where passive seismic imaging was performed in California from seismic noise at stations separated by hundreds to thousands of kilometers (Shapiro et al., 2005; Sabra et al., 2005a); seismic exploration, where seismic body-wave reflections have been retrieved from noise measurements by an array of three-component geophones laid out in a desert area (Draganov et al., 2007); and oceanography, where both direct and reflected wavefronts have been retrieved from ambient noise crosscorrelation in shallow underwater acoustics (Roux and Kuperman, 2004; Sabra et al., 2005b).

The first Weaver and Lobkis (2001) experimental result was interpreted theoretically by invoking equipartitioning of the modes excited in the aluminum sample. A spectral representation (Lobkis and Weaver, 2001), the fluctuation-dissipation approach (Weaver and Lobkis, 2001, 2003; van Tiggelen, 2003; Godin, 2007), or a correlation representation theorem (e.g., Wapenaar, 2004) yields rigorous theoretical approaches to interpreting experimental results in opened complex media. Cases of nonreciprocal (e.g., in the presence of a flow) or inelastic media have also been investigated (Wapenaar, 2006; Godin, 2007; Colin de Verdière, 2006a, 2006b).

For the problem of elastic waves, it has been shown theoretically that the convergence of noise correlation to the Green's function is bonded by the equipartition condition of the different components of the elastic field (Sánchez-Sesma and Campillo, 2006; Sánchez-Sesma et al., 2008). In other words, the emergence of the Green's

Manuscript received by the Editor 8 February 2008; revised manuscript received 9 June 2008; published online 5 November 2008; corrected version published online 20 November 2008.
[1]Université Joseph Fourier, Laboratoire de Géophysique Interne et de Tectonophysique, CNRS, Grenoble, France. E-mail: pierre.gouedard@ujf-grenoble.fr; philippe.roux@obs.ujf-grenoble.fr; michel.campillo@ujf-grenoble.fr.
[2]Shell International Exploration and Production B.V, Rijswijk, The Netherlands. E-mail: arie.verdel@shell.com.

function is effective after a sufficient self-averaging process that is provided by random spatial distribution of the noise sources when considering long time series as well as scattering (Campillo, 2006; Larose et al., 2006; Gouédard et al., 2008).

In some theoretical approaches, Huygens's principle is used to replace the 3D-distributed ambient noise (Roux et al., 2005) by a distribution of sources on a surface surrounding the medium (Wapenaar et al., 2005). As a matter of fact, this result has been demonstrated where experimental randomization is not produced by the distribution of sources but is provided by multiple scattering in heterogeneous media (Campillo and Paul, 2003). By summing the contributions of a spatially uniform distribution of sources to the correlation, it has been shown numerically that the correlation contains the causal and acausal Green's function of the medium (Wapenaar, 2004). Derode et al. (2003a, 2003b) propose to interpret the Green's function reconstruction in terms of a time-reversal analogy and show that correlation of multiply scattered waves could be used for passive imaging in acoustics. Regarding the physics, the convergence of the correlation function toward the Green's function in an unbounded medium finds a natural interpretation through the stationary-phase theorem (Snieder, 2004).

Following these numerical results, we experimentally investigate the link between the spatial distribution of sources and the two-point correlation function when direct waves and multiply scattered waves are supported by the propagation medium. Our objective is to determine the source distribution to retrieve the Green's function for direct and diffuse wavefields. We take advantage of an extensive seismic-prospecting experimental data set where 1600 seismic sources and receivers were deployed on a 25×25-m cell grid, as described in the following section. In the next section, we show the influence of scattering and source distribution on the convergence toward the Green's function. The last section is devoted to reconstructing relative amplitudes of the Green's function with correlation.

THE SEISMIC NETWORK

Petroleum Development Oman (PDO) recorded a high-resolution survey in northern Oman. The data were obtained in a 1×1-km area covered with 1600 geophones located on a 25×25-m cell grid. During this active-seismic survey, vibrators were located on a similar grid shifted with respect to the receiver grid by half a cell (12.5 m) in both directions. The complete data set was then made of 1600×1600 source-receiver time-domain signals constituting an exhaustive measurement of the transfer function of the half-space medium over a 1-km^2 area.

We first selected sources located on a 600-m-internal-diameter, 70-m-wide ring centered on a receiver (Figure 1a). For a given recording time at this receiver, waves from each source were in the same scattering regime because the source-receiver distance was about the same for each source. Figure 1b shows the intensity received at the receiver averaged over all sources in the ring. The shallow subsurface appears to be heterogeneous, and the 4-s records include seismic coda. Direct surface waves arrived in about 0.4 s, which corresponds to a 1000-m/s average speed in the 15–45-Hz frequency bandwidth. At times greater than 1.5 s, the energy decay was linear in decibel scale. This indicated the multiple scattering regime of coda waves. An experimental study had shown that the mean free path in this area was around 1 km in this frequency range. Selecting a time window in the recorded signals was a way to choose the number of scattered waves in the correlation process.

Correlation is equivalent to seismic interferometry (Schuster et al., 2004) when it is performed with direct waves and correlated sources; correlation resembles coda-wave interferometry when the diffuse field from uncorrelated sources is involved. In the following, we focus on surface waves, which are the predominant direct arrivals on the seismograms and play a major part in the coda (Hennino et al., 2001; Campman et al., 2005, Herman and Perkins, 2006).

CORRELATION FUNCTIONS VERSUS SOURCE DISTRIBUTION

From this data set, we select a pair of receivers 158 m apart with a midpoint that coincides with the center of the ring in Figure 1. This ensures the same scattering regime for both receivers at a given recording time. Integrating over a line surrounding the receiver pair is theoretically sufficient to get the Green's function because in our case the medium is lossless (see final section), but we select sources inside a ring to increase the signal-to-noise ratio (S/N) when computing the crosscorrelation. We define the azimuth with respect to the receiver pair, denoted by θ, as the difference between the azimuth defined by one source and the receiver pair center, on one hand, and the receiver pair azimuth on the other (Figure 2). The goal is to compare the convergence of the two-point correlation function to the actual Green's function for different sets of source locations and different amounts of scattering governed by the selected time window. In fact, we consider two time windows. We study the contribution of direct arrivals to the correlation function in the 0–1.5-s interval and the contribution of coda waves in the 1.5–3-s time window.

No processing is performed on the signals, such as frequency whitening or one-bit amplitude-only time-domain equalization. However, to cancel the intensity decay with time in the coda, the logarithmic decrease of the record amplitudes at times greater than 1.5 s is compensated.

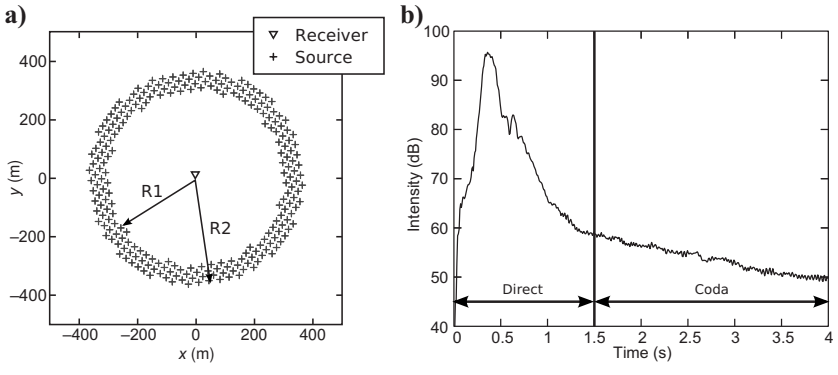

Figure 1. (a) Experimental geometry when considering sources surrounding one receiver. Here, 240 sources were selected, located between two circles of radius $R1 = 300$ m and $R2 = 370$ m, centered on the receiver. (b) Intensity received at the receiver averaged over the sources selected in (a), in decibel scale.

We define the endfire lobes (EFLs) of the receiver pairs as the areas located in the alignment of the receivers (one on each side), with an aperture depending on the ratio between wavelength and range between receivers (Figure 2) (Roux and Kuperman, 2004). We define the aperture of the EFLs as the misalignment of the source with respect to the receiver pair, that causes a delay between the apparent traveltime between the two receivers and the actual Green's function traveltime of 1/8 of a period. In other words, the EFLs are areas in which the phase of the correlation function of direct waves is stationary with respect to azimuth θ. Because the angular aperture of the areas with sources inside or outside the EFLs is different (Figure 2), we adjust the $R1$ and $R2$ radii of the two circles to keep the same number of sources in each area. By doing so, we get comparable S/N in the correlation function, which is more convenient for comparing results.

To improve averaging over sources, and thus S/N of the two-point correlation function, and to ensure a laterally homogeneous medium, we perform an azimuthal average. This is done by considering 17 other receiver pairs, centered on the same point and spaced by the same distance but aligned in other directions θ. For each receiver pair, $R1$ and $R2$ remain the same but θ is redefined according to the receiver pair direction; the set of sources located inside the EFLs is updated.

In Figure 3, we compute the crosscorrelation function between signals from each source of Figure 1a and for two time windows (0–1.5 s and 1.5–3 s). We use a normalized version of the crosscorrelation such that the crosscorrelation $s_{SA} \otimes s_{SB}$ between two traces s_{SA} and s_{SB} recorded for the same sources S at two receivers A and B is divided by the square root of the traces' energies E_{SA} and E_{SB}:

$$C^S_{AB}(t) = \frac{s_{SA} \otimes s_{SB}}{\sqrt{E_{SA}E_{SB}}}(t). \quad (1)$$

The amplitude of the crosscorrelation is thus a correlation coefficient as a function of the time shift. When using direct waves, the crosscorrelation function is highly dependent on source position, whereas the crosscorrelation is independent of source position when using scattered waves. However, the S/N of the crosscorrelation function is much lower for scattered waves than for direct waves.

As a reference signal (i.e., the actual Green's function) for a given receiver pair (A,B) we used the closest source S_B to B recorded by the receiver in A ($G_{BA}(t)$) for positive times and the closest source S_A to A recorded in B ($G_{AB}(t)$) for negative times. To improve the comparison between this reference signal and the two-point correlation function $C_{AB}(t)$, we modified the time axis slightly to correct for the difference between the distances AB and AS_B as well as the difference between AB and S_AB. This 12.5-m distance correction is small compared to the 80-m central wavelength. The amplitude of the reference signal for negative times was also reversed because the relation we expect when averaging the crosscorrelation over sources is (Gouédard et al., 2008)

$$-\frac{d}{dt}\sum_S C^S_{AB}(t) \propto G_{BA}(t) - G_{AB}(-t). \quad (2)$$

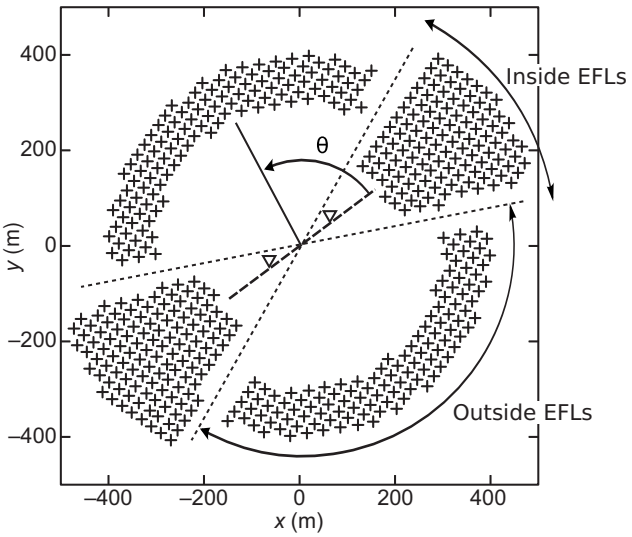

Figure 2. The two geometries we considered, based on θ. The first is $|\theta| < 20°$ and $180 - |\theta| < 20°$, for which sources are inside the EFLs of the receiver pair. The second is $150° > |\theta| > 30°$, for which sources are outside the endfire lobes. In both cases, radii $R1$ and $R2$ are changed to 200–515 m and 300–400 m, respectively, to include the same number of sources as in Figure 1a.

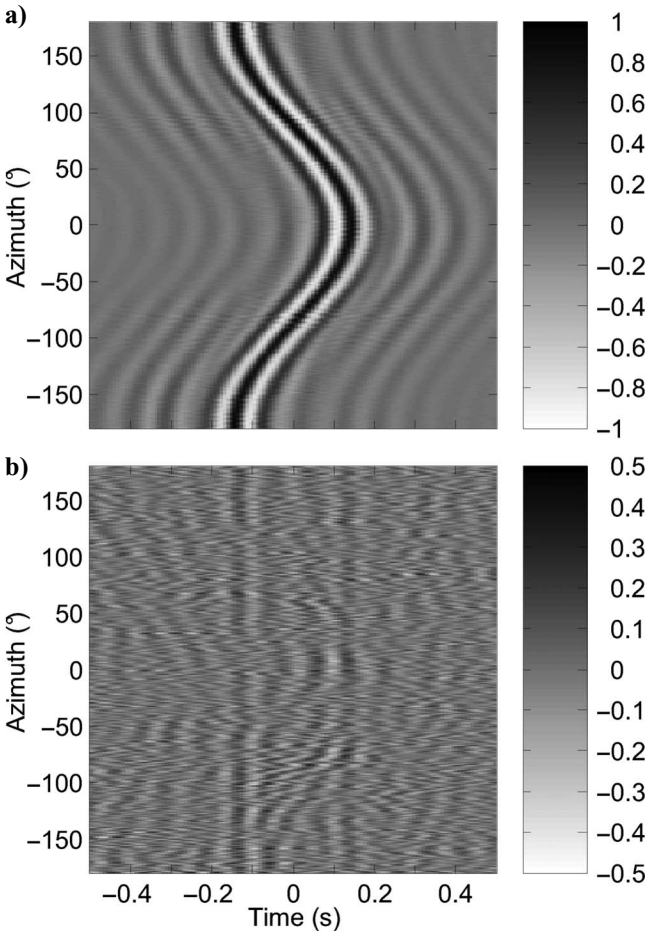

Figure 3. Crosscorrelation function obtained from each source and plotted as a function of azimuth θ for two different time windows, (a) 0–1.5 s and (b) 1.5–3 s. Note the difference in the shading between the two figures.

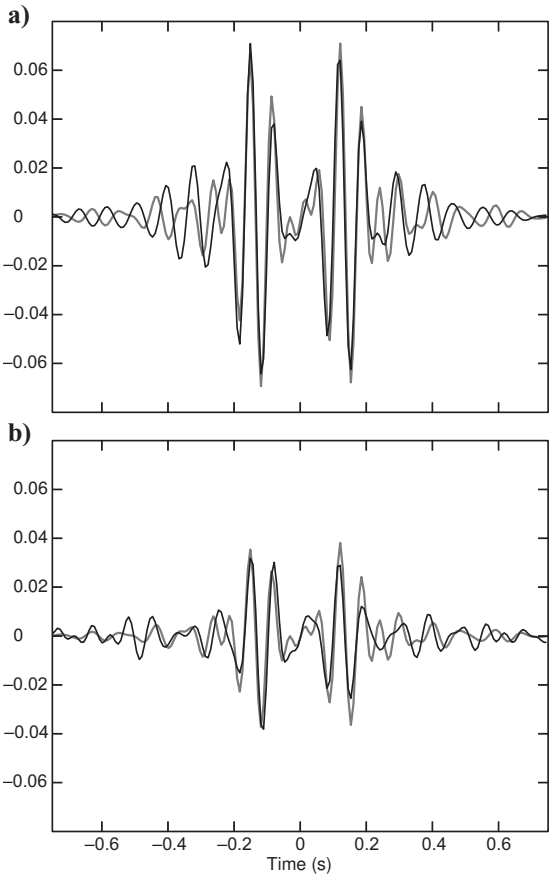

Figure 4. Reconstructed Green's functions for the two time windows, (a) 0–1.5 s and (b) 1.5–3 s, when averaging correlation functions of Figure 3 (black lines). The gray lines reference Green's functions, scaled to the amplitude of the crosscorrelation function for better comparison. Both direct and coda waves yield very good reconstructions of the Green's function.

Figure 5. Crosscorrelation functions averaged over all sources (black line) and reference trace (gray line) for early and late time windows and different source distributions: (a) sources inside the EFLs, 0–1.5 s; (b) sources inside the EFLs, 1.5–3 s; (c) sources outside the EFLs, 0–1.5 s; (d) sources outside the EFLs, 1.5–3 s. In each plot, the reference trace is scaled to the amplitude of the crosscorrelation function for better comparison. When using direct waves (early time window), source locations are important and the Green's function is retrieved only if sources lay inside the EFLs. On the opposite, when using the scattered waves of the coda (late time window), source locations have no influence and the result is similar for both source distributions.

Figure 3a shows that when considering direct arrivals, the crosscorrelation function is highly dependent on the source azimuth. When stacking contributions of all sources (that is, all azimuths), all phases are averaged and only contributions of sources inside the EFLs do not vanish. The normalized crosscorrelation is computed independently for each source and the resulting functions are then averaged. It results in the function shown in Figure 4a. For the later time window, we are in the scattering regime, and the crosscorrelation (Figure 3b) is noisy. Nevertheless, we see direct arrivals common to all crosscorrelation functions, around ± 0.1 s. When averaged over all sources, the S/N increases and direct-wave arrivals are quite evident in Figure 4b. Figure 4 shows that in both cases, the averaged crosscorrelation function is very close to the actual Green's function plotted in gray.

We crosscorrelate traces from two sets of sources (inside/outside the EFLs; see Figure 2) and using two time windows (0–1.5 s for direct waves and 1.5–3 s for coda waves; see Figure 1b). As we have seen when using direct waves, only contributions of sources located inside the EFLs do not vanish in the averaging process. Thus, considering only those sources should yield the same result, except that the S/N will be better because there is no competition between contributing and noncontributing sources. This is the result shown in Figure 5a. Regarding the opposite function, considering only sources outside the EFLs gives a correlation function that is not the Green's function (Figure 5c). Indeed, the peak that emerges in the correlation function is a consequence of the azimuthally dependent source selection because averaging does not produce a constructive interference when sources are outside the EFLs. This result clearly indicates the limitation of using the correlation of direct waves to extract the Green's function.

When using coda waves, the azimuthal distribution of incoming waves is no longer controlled by the distribution of sources but by

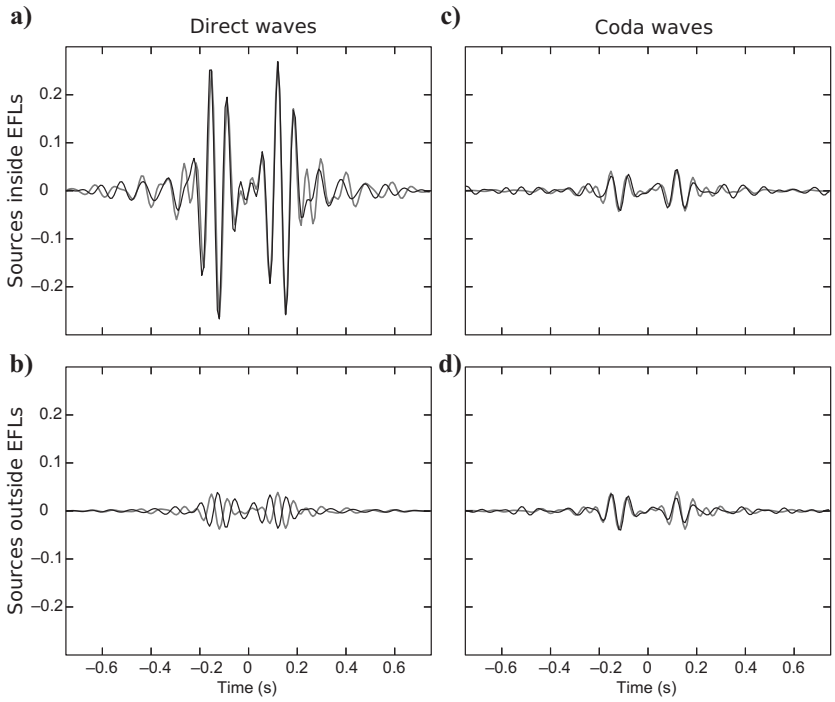

the distribution of scatterers in the medium. When the distribution of scatterers is spatially uniform, coda waves naturally tend to become isotropic. This is illustrated by the correlation functions presented in Figure 5b and d. In Figure 5b, only coda waves produced by sources inside the EFLs are considered. A good agreement between correlation and actual Green's function is reached. The amplitude of the correlation function is lower than for direct waves because only the scattered waves of the coda that travel between the two receivers contribute coherently to the Green's function.

More spectacular is the case shown in Figure 5d, for which coda waves only from sources outside the EFLs are considered. The Green's function is nicely reconstructed, as for sources inside the EFLs. Note that the amplitude of the correlation function is independent of source positions (inside/outside the EFLs) when considering coda waves. This demonstrates the weak sensitivity of local coda waves to the source location, an expected feature for a wavefield evolving toward diffusion. These results confirm the role and importance of scattered waves in the convergence of the correlation function toward the Green's function. This also explains why practical applications are possible even with uneven spatial source distributions.

AMPLITUDE OF THE CROSSCORRELATION FUNCTION

A question that arises about Green's function reconstruction using correlations is how relative amplitudes are retrieved when correlating records from receivers separated by different ranges. As seen, the answer to this question depends on the source distribution and the selected time window in the correlation process. The data set we analyze offers an opportunity to investigate this issue.

Figure 6 shows the experimental geometry used in this section. We select a line of 10 geophones separated by 25 m and another geophone as reference (A) at 50 m, aligned with the geophone line. Correlation functions between the reference and each receiver of the linear array provide the reconstructed Green's function at 10 different ranges from 50 to 275 m. To improve the S/N of the correlation functions, we repeat the process 64 times with the network laterally shifted in both directions, keeping the same experimental interelement geometry. We then measure the amplitude (defined as the maximum of the envelope) of each of the 10 resulting correlation functions. The amplitude-versus-range measurements are compared to the amplitude of records made at each receiver for the closest source to A. For this reference curve, the experimental decay is proportional to the inverse of the source-receiver range. This is from geometric spreading of the surface waves in the near-field regime (here, the wavelength is about 70 m and the maximum source-receiver distance is 275 m).

We measure the amplitude-versus-range curve of the correlation function for different sets of sources (only inside EFLs of each reference/receiver pair, only outside these EFLs, or for all available sources) and two different time windows (0–1.5 s for direct waves or 1.5–3 s for coda waves). Note that EFLs are defined with respect to the actual distance between receivers (Roux and Kuperman, 2004); thus, we consider different sets of sources for each pair, as shown in Figure 6.

Figure 7 shows that relative amplitude with range strongly depends on source distribution and scattering. When considering all sources of the acquisition grid, the amplitude decay with range is similar to the reference curve for both time windows. If we consider direct waves and sources located inside the EFLs only, the amplitude of the correlation does not depend on the range between receivers, as shown in Figure 7a. This can be explained using a time-reversal analogy (Derode et al., 2003a). With the reciprocity principle, the sources inside the EFLs define a limited-aperture time-reversal mirror from which only wave vectors oriented in the direction of the receiver array are reconstructed. Thus, the phase of the correlation function is correct along the receiver array, but the amplitude corresponds to a plane wave.

Using a distribution of sources inside EFLs only could lead to a measure of the medium attenuation because no geometric spreading is expected on the amplitude-versus-range correlation function. Figure 7 shows that attenuation is negligible in the frequency bandwidth of interest in the recorded data. When using coda waves, the source distribution has no influence because waves are scattered. Thus, the correlation function provides the amplitude decay of the reference curve for sources located either inside or outside the EFLs.

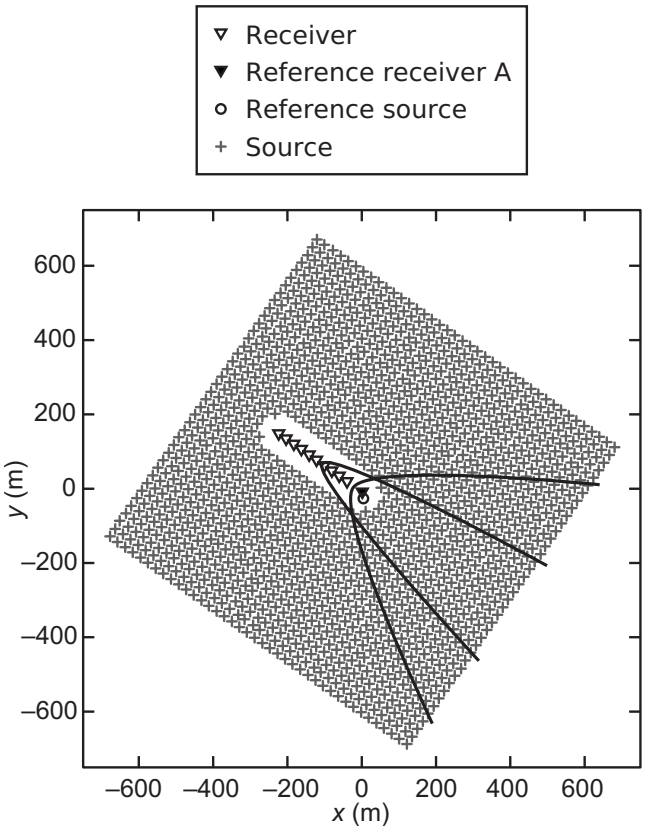

Figure 6. Experimental geometry considered for amplitude measurements. A line of 10 geophones is correlated with one geophone used as a reference (A). The two hyperbola indicate the EFL boundaries for two receiver pairs, the smallest hyperbola aperture corresponding to the largest offset between receivers and the largest aperture to the smallest offset.

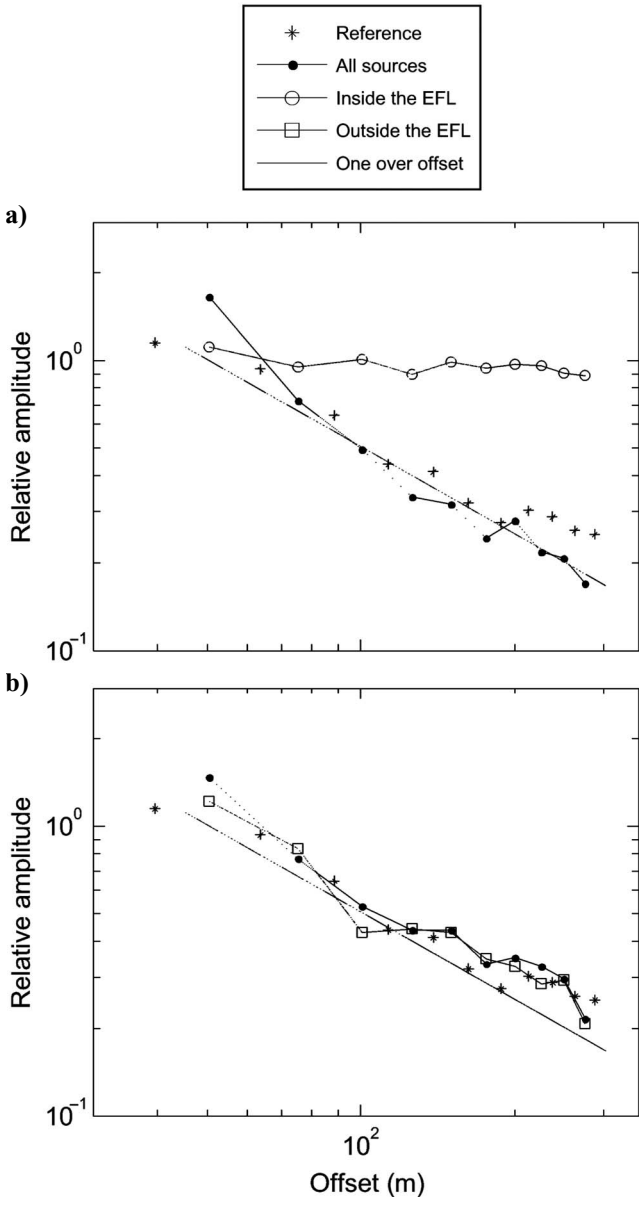

Figure 7. Amplitude-versus-range measured on crosscorrelation functions from different source distributions (all sources as in Figure 6; sources inside the EFLs only or sources outside the EFLs only) and two time windows: 0–1.5 s corresponding to direct waves in (a) and 1.5–3 s corresponding to coda waves in (b). Diamonds are amplitudes measured in the real data from the reference source. Dashed gray lines corresponds to a one-over-offset decay.

CONCLUSION

The crosscorrelation of the seismic motions recorded at two points could yield the Green's function between these points. This result is only valid for particular source positions and/or wavefield properties. The data set we use allows us to investigate different cases by comparing the estimated Green's function obtained using correlation with the actual Green's function using different sets of source locations and different time windows. When using direct waves, source positions govern the convergence of the correlation function toward the Green's function. For coda waves, the source distribution has little influence, and the Green's function can be retrieved in any case. In the reconstructed Green's function, not only the phase but also relative amplitudes for receivers at different offsets are retrieved. This last result is true only for an isotropic wavefield, resulting from an even distribution of sources or from multiply scattered waves. When the source distribution is limited to EFLs, the correlation process only reconstructs a plane wave propagating in the receiver direction; amplitude decay with range no longer includes geometric spreading.

ACKNOWLEDGMENTS

This work was part of a collaboration between Shell and University Joseph Fourier, Grenoble, initiated by the late Gérard Herman. His support and his inspiration are greatly acknowledged. The authors thank the Ministry of Oil and Gas of the Sultanate of Oman and Shell Research for permission to publish these results.

REFERENCES

Aki, K., 1957, Space and time spectra of stationary stochastic waves with special reference to microtremors: Bulletin of the Earthquake Research Institute, **35**, 415–456.

Campillo, M., 2006, Phase and correlation in 'random' seismic fields and the reconstruction of the Green function: Pure and Applied Geophysics, **163**, 475–502.

Campillo, M., and A. Paul, 2003, Long-range correlations in the diffuse seismic coda: Science, **299**, 547–549.

Campman, X. H., K. van Wijk, J. A. Scales, and G. C. Herman, 2005, Imaging and suppressing near-receivers scattered surface waves: Geophysics, **70**, no. 2, V21–V29.

Claerbout, J. F., 1968, Synthesis of a layered medium from its acoustics transmission response: Geophysics, **33**, 264–269.

Colin de Verdière, Y., 2006a, Mathematical models for passive imaging I: General background: Mathematical Physics, accessed 18 August 18 2008; http://fr.arxiv.org/abs/math-ph/0610043.

———, 2006b, Mathematical models for passive imaging II: Effective Hamiltonians associated to surface waves: Mathematical Physics, accessed 18 August 18 2008; http://fr.arxiv.org/abs/math-ph/0610043.

Derode, A., E. Larose, M. Campillo, and M. Fink, 2003a, How to estimate the Green's function of a heterogeneous medium between two passive sensors? Application to acoustic waves: Applied Physics Letters, **83**, 3054–3056.

Derode, A., E. Larose, M. Tanter, J. de Rosny, A. Tourin, M. Campillo, and M. Fink, 2003b, Recovering the Green's function from field-field correlations in an open scattering medium: Journal of the Acoustical Society of America, **113**, 2973–2976.

Draganov, D., K. Wapenaar, W. Mulder, J. Singer, and A. Verdel, 2007, Retrieval of reflections from seismic background-noise measurements: Geophysical Research Letters, **34**, L04305-1–L04305-4.

Duvall, T. L., S. M. Jefferies, J. W. Harvey, and M. A. Pomerantz, 1993, Time distance helioseismology: Nature, **362**, 430–432.

Gilles, P. M., T. L. Duvall, P. H. Scherrer, and R. S. Bogart, 1997, A subsurface flow of material from the sun's equator to its poles: Nature, **390**, 52–54.

Godin, O. A., 2007, Emergence of the acoustic Green's function from thermal noise: Journal of the Acoustical Society of America, **121**, EL96–EL102.

Gouédard, P., L. Stehly, F. Brenguier, M. Campillo, Y. Colin de Verdière, E. Larose, L. Margerin, P. Roux, F. J. Sánchez-Sesma, N. M. Shapiro, and R. L. Weaver, 2008, Crosscorrelation of random fields: Mathematical approach and applications: Geophysical Prospetcing, **56**, 375–393.

Hennino, R., N. Tégourès, N. M. Shapiro, L. Margerin, M. Campilo, B. A. van Tiggelen, and R. L. Weaver, 2001, Observation of equipartition of seismic waves: Physical Review Letters, **86**, 3447–3450.

Herman, G. C., and C. Perkins, 2006, Predictive removal of scattered noise: Geophysics, **71**, no. 2, V41–V49.

Larose, E., A. Derode, M. Campillo, and M. Fink, 2004, Imaging from one-bit correlation of wide-band diffuse wavefield: Journal of Applied Physics, **95**, 8393–8399.

Larose, E., L. Margerin, A. Derode, B. A. van Tiggelen, M. Campillo, N. M. Shapiro, A. Paul, L. Stehly, and M. Tanter, 2006, Correlation of random wavefields: An interdisciplinary review: Geophysics, **71**, no. 4, SI11–SI21.

Larose, E., P. Roux, and M. Campillo, 2007, Reconstruction of Rayleigh-Lamb dispersion spectrum based on noise obtained from an air-jet forcing:

Journal of the Acoustical Society of America, **122**, 3437–3444.
Lobkis, O. I., and R. L. Weaver, 2001, On the emergence of the Green's function in the correlations of a diffuse field: Journal of the Acoustical Society of America, **110**, 3011–3017.
Paul, A., and M. Campillo, 2001, Extracting the Green function between two stations from coda waves: American Geophysical Union, Fall Meeting, Abstracts, D610.
Rickett, J., and J. F. Claerbout, 1999, Acoustic daylight imaging via spectral factorization; Helioseismology and reservoir monitoring: The Leading Edge, **18**, 957–960.
Roux, P., and W. A. Kuperman, 2004, Extracting coherent wavefronts from acoustic ambient noise in the ocean: Journal of the Acoustical Society of America, **116**, 1995–2003.
Roux, P., K. G. Sabra, W. A. Kuperman, and A. Roux, 2005, Ambient noise cross correlation in free space: Theoretical approach: Journal of the Acoustical Society of America, **117**, 79–84.
Sabra, K. G., P. Gerstoft, P. Roux, W. A. Kuperman, and M. C. Fehler, 2005a, Extracting time-domain Green's function estimates from ambient seismic noise: Geophysical Research Letters, **32**, L03310.
Sabra, K. G., P. Roux, and W. A. Kuperman, 2005b, Emergence rate of the time-domain Green's function from the ambient noise crosscorrelation: Journal of the Acoustical Society of America, **118**, 3524–3531.
Sabra, K. G., A. Srivastava, F. L. di Scalea, I. Bartoli, P. Rizzo, and S. Conti, 2008, Structural health monitoring by extraction of coherent guided waves from diffuse fields: Journal of the Acoustical Society of America, **123**, EL8–EL13.
Sánchez-Sesma, F. J., and M. Campillo, 2006, Retrieval of the Green function from cross correlation: The canonical elastic problem: Bulletin of the Seismological Society of America, **96**, 1182–1191.
Sánchez-Sesma, F. J., J. A. Pérez-Ruiz, F. Luzòn, M. Campillo, and A. Rodriguez-Castellano, 2008, Diffuse fields in dynamic elasticity: Wave Motion, **45**, 641–654.
Schuster, G. T., J. Yu, J. Sheng, and J. Rickett, 2004, Interferometric/daylight seismic imaging: Geophysical Journal International, **157**, 838–852.
Shapiro, N. M., and M. Campillo, 2004, Emergence of broadband Rayleigh waves from correlations of the ambient seismic noise: Geophysical Research Letters, **31**, L07614.
Shapiro, N. M., M. Campillo, L. Stehly, and M. H. Ritzwoller, 2005, High-resolution surface wave tomography from ambient seismic noise: Science, **307**, 1615–1618.
Snieder, R., 2004, Extracting the Green's function from the correlation of coda waves: A derivation based on stationary phase: Physical Review E, **69**, 046610.
van Tiggelen, B. A., 2003, Green function retrieval and time reversal in a disordered world: Physical Review Letters, **91**, 243904.
Wapenaar, K., 2004, Retrieving the elastodynamic Green's function of an arbitrary inhomogeneous medium by crosscorrelation: Physical Review Letters, **93**, 254301.
———, 2006, Nonreciprocal Green's function retrieval by cross correlation: Journal of the Acoustical Society of America, **120**, EL7–EL13.
Wapenaar, K., J. Fokkema, and R. Snieder, 2005, Retrieving the Green's function by crosscorrelation: A comparison of approaches: Journal of the Acoustical Society of America, **118**, 2783–2786.
Weaver, R. L., and O. I. Lobkis, 2001, Ultrasonics without a source: Thermal fluctuation correlations at MHz frequencies: Physical Review Letters, **87**, 134301.
———, 2003, Elastic wave thermal fluctuations, ultrasonic waveforms by correlation of thermal phonons: Journal of the Acoustical Society of America, **113**, 2611–2621.